

UNCLASSIFIED

Defense Technical Information Center
Compilation Part Notice

ADP012229

TITLE: Substrate Dependence in the Growth of Three-Dimensional Gold Nanoparticle Superlattices

DISTRIBUTION: Approved for public release, distribution unlimited

This paper is part of the following report:

TITLE: Nanophase and Nanocomposite Materials IV held in Boston, Massachusetts on November 26-29, 2001

To order the complete compilation report, use: ADA401575

The component part is provided here to allow users access to individually authored sections of proceedings, annals, symposia, etc. However, the component should be considered within the context of the overall compilation report and not as a stand-alone technical report.

The following component part numbers comprise the compilation report:

ADP012174 thru ADP012259

UNCLASSIFIED

Substrate Dependence in the Growth of Three-Dimensional Gold Nanoparticle Superlattices

S. Sato, N. Yamamoto, H. Yao and K. Kimura

Department of Material Science, Himeji Institute of Technology,
3-2-1 Koto, Kamigori-cho, Ako-gun, Hyogo 678-1297 JAPAN

ABSTRACT

Three-dimensional superlattices consisting of gold nanoparticles were grown at air/suspension or suspension/solid interfaces. The growth of superlattices was found to be strongly dependent on substrate materials: Micrometer-sized superlattices were grown at air/suspension interfaces and upon silver substrates, whereas no growth was observed on silicon, silicon oxide, or amorphous carbon substrates. To explain the observed substrate dependence, Lifshitz theory was used to calculate the Hamaker constants between gold nanoparticle assemblies and substrates through the suspension. Van der Waals interactions estimated from this calculation fully explain the experimental results.

INTRODUCTION

Three-dimensional (3D) superlattices of nanoparticles represent a class of promising new electronic materials whose band structures may be engineered through control of core sizes, of surface coverage thicknesses, and of packing arrangements for the nanoparticles. Recently, high-quality superlattices have been synthesized using the self-assembly process of nanoparticles in liquid phases [1-4]. For superlattices to be introduced into industrial applications, they need to be grown at gas/solution or solution/solid interfaces. However, there have been no reports focusing on superlattice growth at various interfaces. Recently, we have found that gold (Au) nanoparticles, whose surfaces are modified with hydrophilic surfactants, are good components for 3D superlattices since the assembly rate of Au nanoparticles (i.e., the growth rate of superlattices) is widely tunable through pH control [5,6]. By enforcing an extremely slow growth rate (i.e., equilibrium growth), Au nanoparticles self-assemble into high-quality lattice arrangements. In this communication, we report substrate dependence in the growth of Au nanoparticle superlattices in aqueous suspensions.

EXPERIMENTAL

The preparation of Au nanoparticles is outlined as follows. 4.1 ml of an aqueous solution of 0.12 M hydrogen tetrachloroaurate tetrahydrate ($\text{HAu(III)Cl}_4 \cdot 4\text{H}_2\text{O}$) was mixed with 100 ml of methanol containing 1.5 mM of mercaptosuccinic acid (MSA). 25 ml of an aqueous solution of 0.2 M sodium borohydride (NaBH_4) was then added under vigorous stirring. After the reaction, Au nanocrystals were obtained whose surfaces were modified with MSA. The solvent was decanted after centrifugation at $9840\times g$, which corresponds to 10,000 rpm for the Kubota 1720 centrifuge. Samples were then washed twice with a 20 % (v/v) water-methanol solution by repeating re-suspension with a sonicator and re-centrifugation, and finally dialyzed to remove inorganic (Na, Cl, and B) and organic impurities.

The surfactant affects the dispersion of Au nanoparticles in aqueous suspensions at low ion concentrations. After the Au nanoparticles were dispersed in distilled water, hydrochloric acid (HCl) was then added into the suspension. This process induced self-assembly of the nanoparticles. This is a

result of the added protons suppressing ionization of the surfactants and hence, weakening repulsive interactions among the nanoparticles. Silver (Ag), silicon (Si), Si oxide, or amorphous carbon (a-C) substrates were immersed in the suspension, and samples were stored in a closed glass bottle to prevent solvent evaporation. Prior to the experiment, the surface oxide of Si substrates was removed by dipping into a 47 wt. % HF solution.

The obtained superlattices were examined with a transmission electron microscope (TEM: Hitachi H-8100) operated at 200 kV, and a scanning electron microscope (SEM: Philips XL-20LaB6) operated at 9 kV.

RESULTS

Growth at air/suspension interfaces

With an appropriate amount of HCl, superlattices appeared at the air/suspension interface within 4 - 10 days. Figure 1 shows TEM images of (a) the overall shapes of the superlattices and (b) an edge of one of the superlattices. Superlattices achieved widths of several micrometers and formed faceted structures as shown in image (a). This indicates that they were grown under equilibrium conditions [7,6]. Image (b) shows that Au nanoparticles form a close-packed arrangement in the superlattices. The diameters of the component nanoparticles are 4.9 nm: The core diameters of the component nanoparticles are 3.5 nm, and the thickness of the surfactants is 0.7 nm.

Growth at suspension/substrate interfaces

After the addition of an appropriate amount of HCl into the suspension, superlattices were grown on

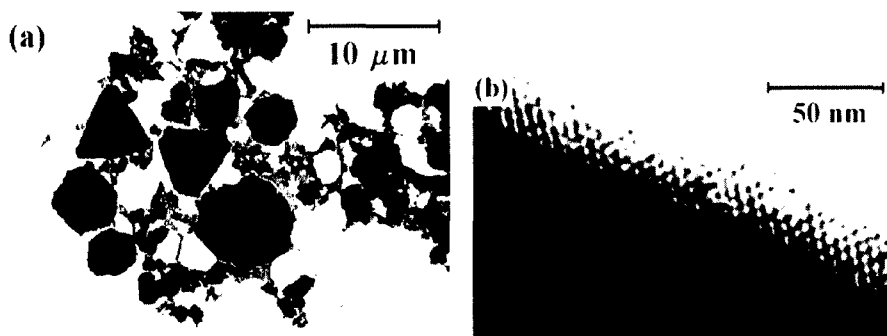


Figure 1. TEM images of superlattices grown at the air/suspension interface: (a) a low magnification image, and (b) a typical image of an edge of the superlattice. The superlattices were prepared with an HCl concentration of 3.6×10^{-1} M.

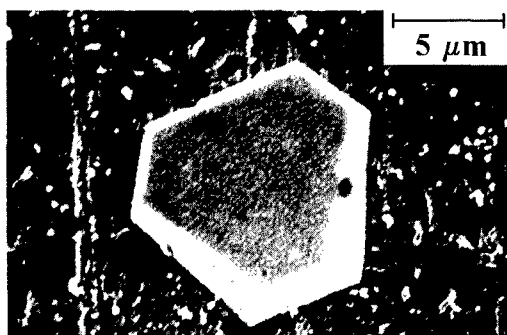


Figure 2. A typical SEM image of a superlattice grown on an Ag substrate. The sample was prepared with an HCl concentration of 3.6×10^{-2} M.

Ag substrates, however, no growth was observed on Si, Si oxide, or a-C substrates. A typical SEM image of a superlattice grown on an Ag substrate is shown in Fig. 2. After sufficient growth, the superlattices spanned several micrometers, and they formed clear facets, indicating formation of the desired superlattices.

DISCUSSION

Throughout this discussion, we will consider interactions between Au nanoparticle assemblies and substrates to determine the observed substrate dependence. Interactions between two materials consist of (1) surface interactions such as Coulombic and hydrophobic interactions; and (2) volume interactions such as the van der Waals interaction [8]. In general, surface interactions are dominant in nanostructured materials as the number of atoms at the surface is significant relative to the volume. However, our experimental results are not fully explained by surface interactions. The attractive interaction between air and the Au nanoparticle assemblies cannot be explained solely by Coulombic interactions. Although this attractive interaction can be explained by hydrophobic interactions, it conflicts with the experimental observation that assemblies are not attracted to other hydrophobic materials, such as hydrogen-terminated Si or a-C. It appears that a volume interaction needs to be taken into account for complete understanding of the observed substrate dependency.

To consider volume interactions, we calculate the Hamaker constants between the Au nanoparticle assemblies and various substrates across water, which describe the attractive or repulsive magnitude of the van der Waals interaction. In Lifshitz theory [8], the Hamaker constant between material 1 and material 2 across medium 3 is given by

$$A \approx \frac{3}{4} kT \left(\frac{\epsilon_1 - \epsilon_3}{\epsilon_1 + \epsilon_3} \right) \left(\frac{\epsilon_2 - \epsilon_3}{\epsilon_2 + \epsilon_3} \right) + \frac{3h}{4\pi} \int_0^\infty \left(\frac{\epsilon_1(i\nu) - \epsilon_3(i\nu)}{\epsilon_1(i\nu) + \epsilon_3(i\nu)} \right) \left(\frac{\epsilon_2(i\nu) - \epsilon_3(i\nu)}{\epsilon_2(i\nu) + \epsilon_3(i\nu)} \right) d\nu, \quad (1)$$

where ϵ_1 , ϵ_2 and ϵ_3 are the static dielectric constants of the three materials, $\epsilon(i\nu)$ are the values of ϵ at imaginary frequencies, and ν_1 is $2\pi kT/h$. Using appropriate forms of $\epsilon(i\nu)$ is the key for successful estimation of the Hamaker constants in the present calculation.

Let us consider what form of $\epsilon(i\nu)$ is suitable for Au nanoparticle assemblies. We will begin by assuming Au nanoparticles as artificial atoms. The conduction electrons in a metal nanoparticle behave not as a relaxator system, but as an oscillator system with an eigenfrequency equal to the surface plasmon frequency of the metal [9]. This means that Au nanoparticles can be likened to atoms of the Thomson model. The number of valence electrons in this artificial atom corresponds to the number of conduction electrons in an Au core: $N_v = (4/3)\pi R^3 n_{Au}$, where R is the radius of the Au core and n_{Au} is the conduction electron density of bulk Au ($5.9 \times 10^{28} \text{ m}^{-3}$). Since MSA is an insulator, the contribution of conduction electrons from MSA to the artificial atom is neglected. Au nanoparticle assemblies are, therefore, likened to virtual dielectrics consisting of those artificial atoms. Assuming that the artificial atoms are simple harmonic oscillators with the eigenfrequency ν_0 , the function $\epsilon(i\nu)$ of the virtual dielectrics is

$$\epsilon(i\nu) = 1 + \frac{n_a N_v e^2}{4\pi^2 \epsilon_0 m} \cdot \frac{1}{\nu_0^2 + \nu^2 + i\nu\Gamma/(2\pi)}, \quad (2)$$

where n_a is the number density of the artificial atoms in a virtual dielectric and Γ is the damping factor. We set the number density, n_a , to the value at which nanoparticles form closest-packing arrangements. From optical studies of our superlattices [10], the surface plasmon frequency ν_0 , the damping factor Γ , and the optical mass m were estimated to be $4.6 \times 10^{14} \text{ sec}^{-1}$, $1.4 \times 10^{15} \text{ sec}^{-1}$, and $2.5 m_e$ (m_e : mass of free electrons), respectively. The static dielectric constant of the virtual dielectric was estimated by substituting 0 for ν in Eq. 2. For $\epsilon(i\nu)$ of Ag, Si, SiO_2 , and a-C substrates and water, we used the equations shown in Ref. 8. In addition to those substrates, we also analyzed AgCl substrates since the surface of our Ag substrates may be chloridized as a result of the HCl addition. Physical parameters to construct $\epsilon(i\nu)$ of SiO_2 and water are listed in Ref. 8. For other substrates, the following parameters are used, the static dielectric constant, the refractive index, and the main electronic absorption frequency of Si are 12, 3.5, and $1.0 \times 10^{15} \text{ sec}^{-1}$, respectively [11], and those of AgCl are 11, 2.1, and $1.2 \times 10^{15} \text{ sec}^{-1}$, respectively [12, 13]; The volume plasmon frequency of Ag is $9.1 \times 10^{14} \text{ sec}^{-1}$ [14], and that of a-C is $6.3 \times 10^{15} \text{ sec}^{-1}$ [14].

Using all of the above equations and parameters, interactions between the virtual dielectrics, which represent Au nanoparticle assemblies, and the substrates were calculated. Figure 3 shows the calculated Hamaker constants as a function of the diameters of component nanoparticles. The positive and negative values correspond to attractive and repulsive interactions, respectively. The Hamaker constants at the diameter of the component particles, 4.9 nm, predict the following interactions. Au nanoparticle assemblies are attracted to the air and Ag substrates, but repulsed from SiO_2 , Si and a-C substrates. These results perfectly explain the experimental results. The interaction between Au nanoparticle assemblies and AgCl is almost neutral at 4.9 nm. Thus, even if an AgCl layer is grown on the Ag surface, the layer does not inhibit the attractive interaction between Au nanoparticle assemblies and Ag substrates.

It is quite surprising that the experimental results are fully explained without the consideration of surface interactions. This may indicate that our proton density in the aqueous suspensions was appropriate for neutralizing hydrophilicity/hydrophobicity as well as suppressing Coulombic interactions. In the present experiment, an extremely slow growth rate for the superlattices was tuned by adjusting the HCl concentration. Thus, the proton density was adjusted to balance attractive and

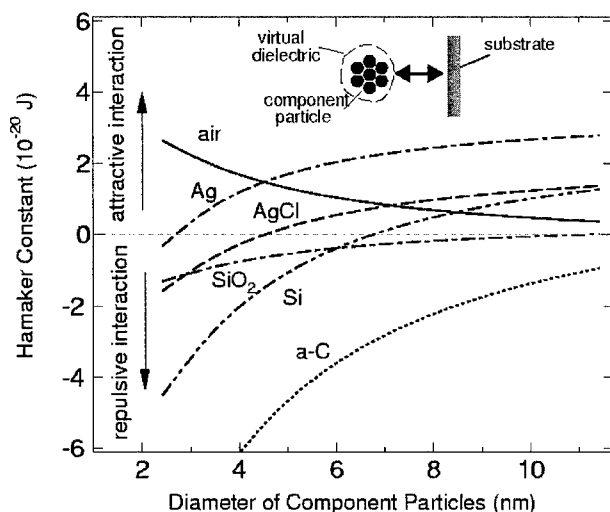


Figure 3. Substrate dependency of the Hamaker constants between the virtual dielectrics and various substrates through water as a function of the diameters of component nanoparticles. The virtual dielectrics represent the close-packing assemblies of Au nanoparticles.

repulsive interactions between the nanoparticles. This adjustment may prove to be a general procedure by which the surface interactions of MSA monolayers become insignificant. To verify this hypothesis, an investigation of the pH dependence of surface forces of MSA monolayers is currently underway.

CONCLUSIONS

We investigated substrate dependence in the growth of Au nanoparticle superlattices in aqueous suspension. Superlattice growth proceeded at the air/suspension interface and the suspension/Ag interface. After sufficient growth, the superlattices reached widths of several micrometers and formed clear facets. In contrast, no growth was observed on Si, SiO₂, and a-C substrates. The observed substrate dependency was not explained by surface interactions but by the van der Waals interaction. The Hamaker constants between Au nanoparticle assemblies and substrates through water were calculated using the Lifshitz theory. In the calculation, Au nanoparticle assemblies were assumed as virtual dielectrics consisting of artificial atoms of Thomson model. The calculation results well explained the experimental observations.

ACKNOWLEDGEMENTS

This study was supported by the Hosokawa Powder Technology Foundation, the Mitsubishi Research Institute, and the Japan Space Utilization Promotion Center.

REFERENCES

1. A. Taleb, C. Petit and P. Pileni, *Chem. Mater.* **9**, 950 (1997).
2. S. A. Harfenist, Z. L. Wang, M. M. Alvarez, I. Vezmar and R. L. Whetten, *J. Phys. Chem.* **100**, 13904 (1996).
3. C. B. Murray, C. R. Kagan and M. G. Bawendi, *Annu. Rev. Mater. Sci.* **30**, 545 (2000).
4. C. P. Collier, T. Vossmeier and J. R. Heath, *Annu. Rev. Phys. Chem.* **49**, 371 (1998).
5. K. Kimura, S. Sato and H. Yao, *Chem. Lett.* 372 (2001).
6. S. Sato, N. Yamamoto, H. Yao and K. Kimura, (to be published).
7. A. Zangwill, *Physics at Surfaces* (Cambridge University Press, Cambridge, 1988) pp. 12 - 15.
8. J. Israelachvili, *Intermolecular and Surface Forces* (Academic Press, London, 1992).
9. U. Kreibig, and M. Vollmer, *Optical Properties of Metal Clusters* (Springer-Verlag, Berlin, 1995) pp. 23 - 25.
10. S. Sato, H. Yao and K. Kimura, (to be published).
11. S. Adachi, *Optical Constants of Crystalline and Amorphous Semiconductors* (Kluwer Academic Publishers, Boston, 1999) pp. 18 - 32.
12. D. R. Lide, *CRC Handbook of Chemistry and Physics*, 77th ed. (CRC press, Boca Raton, 1996) p. 12-45.
13. H. Kanzaki, *Photo. Sci. Eng.*, **24**, 219 (1980).
14. H. Raether, *Excitation of Plasmons and Interband Transitions by Electrons* (Springer-Verlag, Berlin, 1980) pp. 51 - 52.